Plant Physiology and Biochemistry 47 (2009) 1061–1068

Contents lists available at ScienceDirect

Plant Physiology and Biochemistry

journal homepage: www.elsevier.com/locate/plaphy

Research article

Biochemical and physiological characterization of a tau class glutathione transferase from rice (*Oryza sativa*)

Xue Yang [a,b], Wu Sun [a,b], Jiang-Peng Liu [a,b], Yan-Jing Liu [a], Qing-Yin Zeng [a,*]

[a] State Key Laboratory of Systematic and Evolutionary Botany, Institute of Botany, Chinese Academy of Sciences, Beijing 100093, China
[b] Graduate School, Chinese Academy of Sciences, Beijing 100049, China

ARTICLE INFO

Article history:
Received 27 November 2008
Accepted 6 July 2009
Available online 15 July 2009

Keywords:
Glutathione transferase
Enzyme activity
Rice (*Oryza sativa*)
Abiotic stress

ABSTRACT

The classical phase II detoxification glutathione transferases (GSTs) are key metabolic enzymes that catalyze the conjugation of glutathione to various electrophilic compounds. A tau class GST gene (*Os*GSTU17) was cloned from rice, which encodes a protein of 223 amino acid residues with a calculated molecular mass of 25.18 kDa. The recombinant *Os*GSTU17 formed a homodimer protein and showed GSH-conjugating activity with various xenobiotics. Kinetic analysis with respect to NBD-Cl as substrate revealed a K_m of 0.324 mM and V_{max} of 0.219 μmol/min per mg of protein. The enzyme had a maximum activity at pH 7.5, and a high thermal stability with 81% of its initial activity at 55 °C for 15 min. Site-directed mutagenesis revealed that Ser15 in the N-terminal domain is a critical catalytic residue, responsible for stabilisation of the thiolate anion of enzyme-bound glutathione. *Os*GSTU17 mRNA was expressed in different tissues of rice, both above and below ground. The relative transcript levels of *Os*GSTU17 mRNA varied significantly among the tissues in response to CDNB, hydrogen peroxide and atrazine treatments, indicating the gene has diverse regulation mechanisms in response to abiotic stresses.

1. Introduction

Glutathione transferases (GSTs; EC 2.5.1.18) are soluble dimeric proteins that catalyze the conjugation of the tripeptide glutathione (ã-glutamyl-cysteinyl-glycine; GSH) to a number of electrophilic, lipophilic compounds, forming a water-soluble product. This reaction has been demonstrated to play a central role in the detoxification of many toxic molecules, including carcinogens, pesticides and herbicides, in a wide range of species from mammals to insects and plants [1,2]. Based on protein sequence similarity and immunological cross-reactivity, eight classes of mammalian GSTs have been recognized: Alpha, Kappa, Mu, Pi, Theta, Sigma, Zeta and Omega [3]. In plant, GSTs are mainly grouped into six classes, phi, zeta, tau, theta, lambda and DHAR (dehydroascorbate reductases) [4]. The zeta and theta GSTs are found both in plants and animals, but the tau and phi GSTs are considered as unique to plants [4]. In plants, tau GST activity protects cells from a wide range of biotic and abiotic stresses [5–9]. Recently, plant tau class GST has been considered to be in regulation of cell elongation and flowering in response to light [10].

Plant GSTs have been extensively studied because of their ability to detoxify chemically diverse herbicides and heavy metal toxins. Individual GSTs conferring herbicide tolerance have been characterized in rice, maize, wheat and other plant species [6,11–15]. Rice (*Oryza sativa*) is one of the most important cereal crops in the world, providing food for more than half the world's population. Genome analysis has identified 61 GST sequences, among which 40 are the plant-specific tau class GSTs [16]. The function of these tau GSTs in rice remain little studied. Up to today, only three tau GST isozymes have been characterized in rice [17,18]. The molecular and functional characterization of each GST members are needed to understand their functional significance and the role in developmental processes and herbicide detoxification of this important crop. In this study, we cloned and biochemically characterized a tau GST (*Os*GSTU17) from rice. Quantitative expression analysis revealed this gene was responsive to different abiotic stress treatments. In addition, the *Os*GSTU17 protein showed GSH-conjugating activity with various xenobiotics, suggesting its possible role in detoxification.

2. Results and discussion

2.1. Sequence characterization of the *OsGSTU17* gene

A single fragment of *Os*GSTU17 cDNA was amplified by the primers *Os*GSTU17-EX1/OsGSTU17-EX2. The full nucleotide and deduced amino acid sequences are shown in Fig. 1. The *Os*GSTU17 cDNA contained a 669 bp open reading frame (excluding the stop codon),

* Corresponding author. Tel.: +86 10 62836440; fax: +86 10 62590843.
E-mail address: qingyin.zeng@ibcas.ac.cn (Q.-Y. Zeng).

0981-9428/$ – see front matter © 2009 Elsevier Masson SAS. All rights reserved.
doi:10.1016/j.plaphy.2009.07.003

```
ATGGCAGCAGACAAGGGAGTGAAGGTGTTCGGCATGTGGGCGAGCCCCATGGCGATCCGT
 M  A  A  D  K  G  V  K  V  F  G  M  W  A  S  P  M  A  I  R
GTGGAGTGGGCGCTCCGGCTCAAGGGCGTCGACTACGAGTACGTCGACGAGGACCTCGCC
 V  E  W  A  L  R  L  K  G  V  D  Y  E  Y  V  D  E  D  L  A
AACAAGAGCGAGGCGCTGCTCCGGCACAACCCGGTGACCAAGAAGGTGCCCGTGCTGGTC
 N  K  S  E  A  L  L  R  H  N  P  V  T  K  K  V  P  V  L  V
CACGACGGCAAGCCTCTCGCCGAGTCCACCGTCATCGTCGAGTACATCGACGAGGCCTGG
 H  D  G  K  P  L  A  E  S  T  V  I  V  E  Y  I  D  E  A  W
AAGCACGGCTACCCCATCATGCCCTCCGACCCCTTCGACCGTGCTCAGGCGAGGTTCTGG
 K  H  G  Y  P  I  M  P  S  D  P  F  D  R  A  Q  A  R  F  W
GCCAGGTTCGCTGAAGAGAAGgtataatccaactttctctactgatgactcaaatccaaa
 A  R  F  A  E  E  K
tccaatccttttttttttctgacctcttagttagattgattggctttgcattggaaaagtg
atttcatcactcggggatatcccctcccctcgtttttacatgacatctaaatagtcata
agaaaatttggtaacatagattaatataaaatatatcactccacaaacatgcaatttaa
atttaatttctacaagttgtaacaaaaataacaaatatagctgcgaatgtacgataacta
ttttcagtttaatttatttttttttgttgcaagttgtataagttgaatttattgaatttt
gtatagcatgtctgtggagtgatatatttcatagtattaatctatgttgttaattttttt
aataactatatagatgatatacaaacaagaggatattcccttgagaaatgaaaatccacg
ttcctttacgttgcattggatgttgttatagTGCAACGCTGCTCTGTACCCGATCTTCAT
                                C  N  A  A  L  Y  P  I  F  M
GACGACCGGAGAGGAGCAGAGAAAGCTGGTGCACGAGGCCCAGCAGTGCCTGAAGACGCT
  T  T  G  E  E  Q  R  K  L  V  H  E  A  Q  Q  C  L  K  T  L
GGAGACGGCCCTGGAGGGGAAGAAGTTCTTCGGCGGCGACGCCTTCGGCTACCTTGACAT
  E  T  A  L  E  G  K  K  F  F  G  G  D  A  F  G  Y  L  D  I
CGTCACCGGGTGGTTCGCCTACTGGCTGCCGGTCATCGAGGAGGCCTGCGGCGTCGAAGT
  V  T  G  W  F  A  Y  W  L  P  V  I  E  E  A  C  G  V  E  V
CGTCACCGACGAGGCGCTGCCCCTGATGAAGGCCTGGTTCGACCGGGTCCTCGCCGTCGA
  V  T  D  E  A  L  P  L  M  K  A  W  F  D  R  V  L  A  V  D
CGCCGTGAAGGCGGTCCTGCCGCCGAGGGACAAGCTCGTCGCGCTCAACAAGGCTCGCCG
  A  V  K  A  V  L  P  P  R  D  K  L  V  A  L  N  K  A  R  R
TGAGCAGATCCTCTCGGCGTAG
  E  Q  I  L  S  A  *
```

Fig. 1. Nucleotide sequence and deduced amino acid sequence of the *Os*GSTU17. Stop codon is denoted by an asterix. The intron sequence is in lower case.

which encodes a peptide of 223 residues that has a predicted molecular weight (*Mw*) of 25.18 kDa. The nucleic acid sequence of this cDNA was identical to the putative glutathione transferase *Os*GSTU17 mRNA (GenBank accession no. AF402804) [16]. Phylogenetic analysis of the protein sequences placed *Os*GSTU17 in the tau class GSTs with strong bootstrap support (Fig. 2). The intron/extron numbers are conserved among members of the same GST subfamily [3]. Plant tau type GST genes have a single intron [3]. By comparison of the genomic sequence (Os09g0467200) and the cDNA sequence, *Os*GSTU17 revealed a 490 bp intron (Fig. 1), similar to the gene structure of other plant tau class GSTs. Thus, based on the amino acid sequence similarity and gene structure features, *Os*GSTU17 should be classified as a tau class GST.

The sequence of *Os*GSTU17 protein was used in a homology analysis with the BLAST program (http://www.ncbi.nlm.nih.gov/BLAST). The protein sequence showed a high similarity to other plant tau GST proteins. A multiple sequence alignment of the *Os*GSTU17 protein with other plant GSTs is shown in Fig. 3. *Os*GSTU17 showed 33–46% sequence identity to plant tau GSTs listed in Fig. 3. Much higher sequence similarity (56%) was observed in the N-terminal domain than in the C-terminal domain (29%).

2.2. Biochemical characterization of the recombinant *OsGSTU17*

Recombinant *Os*GSTU17 was over-expressed in *E. coli* BL21 transformed with plasmid ΔpET30a/OsGSTU17 (Fig. 4, lane 7). SDS–PAGE of the bacterial cells induced by IPTG at 37 °C revealed that the majority of the expressed proteins were present in the supernatant (Fig. 4, lane 9). The subunit *Mw* of the recombinant *Os*GSTU17, as deduced from the amino acid sequence, should be 26.4 kDa (include 6×His-tag). MALDI-TOF/MS confirmed the subunit *Mw* of the recombinant *Os*GSTU17 was 26.4 kDa (Fig. 5A). The *Mw* of the purified recombinant *Os*GSTU17 was estimated to be approximately 52 kDa according to Sephadex G-75 gel filtration (results not shown). Thus, the recombinant *Os*GSTU17 is considered to be a homodimer similar to rice *Os*GSTU5 and other plant tau GSTs [18–20].

The catalytic activities of the recombinant *Os*GSTU17 towards various substrates are presented in Table 1. *Os*GSTU17 had higher activity towards NBC than to NBD-Cl and CDNB, and no activity towards substrate DCNB, 4-NPA and ECA. CDNB is a classical GST substrate and is used widely in the detection and determination of GST activity. Compared to another rice tau GST *Os*GSTU5, which has an activity of 4.48 μmol/min per mg towards CDNB [18], *Os*GSTU17's CDNB conjunction activity was low. The cumene hydroperoxide activity of *Os*GSTU17 is similar to tomato tau class GSTs *Le*GSTU3-3 and *Le*GSTU5-5, but much lower than other tomato and wheat tau class GSTs (*Le*GSTU1-1, *Le*GSTU2-2, *Le*GSTU4-4, *Ta*GSTU1-1, *Ta*GSTU4-4) [6,21].

The apparent kinetic constants of the *Os*GSTU17 were determined using NBD-Cl and GSH as substrates. The apparent $K_m^{\text{NBD-Cl}}$ value of *Os*GSTU17 was found to be 0.324 mM (Table 2), similar to tomato tau class GST *Le*GSTU3-3 [21]. The K_m^{GSH} of *Os*GSTU17 for GSH was 0.058 mM, which is much lower than that of other published plant GSTs [18,22,23], indicating that *Os*GSTU17 has high affinity for GSH. In enzyme-catalyzed reactions, the specificity constant k_{cat}/K_m reflects catalytic efficiency. The k_{cat}/K_m value of *Os*GSTU17 for the substrates NBD-Cl and GSH were 0.793 and 4.552, respectively (Table 2). Although *Os*GSTU17 showed a relatively high affinity for GSH, compared to other plant GSTs the catalytic efficiency of *Os*GSTU17 is low.

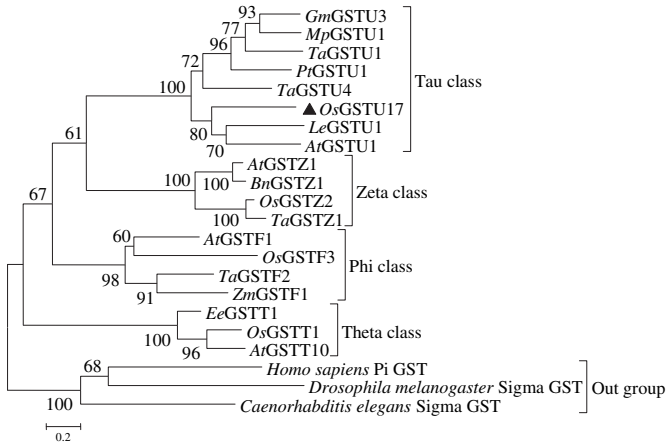

Fig. 2. Phylogenetic relationships between *Os*GSTU17 and other classes of plant GSTs. The neighbour-joining method was used in the tree reconstruction. Bootstrap values from a sample of 1000 replicates are shown on each branch. The tree was rooted with *Caenorhabditis elegans* Sigma GST (GenBank accession number P91252), *Drosophila melanogaster* Sigma GST (GenBank accession number P41043) and *Homo sapiens* Pi GST (GenBank accession number P09211). The affiliations of the plant GST sequences used in the tree reconstruction are the following: *Gm*GSTU3 (*Glycine max*, GenBank accession number X68819); *Mp*GSTU1(*Malva pusilla*, GenBank accession number AY206001); *Ta*GSTU1 (*Aegilops tauschii*, GenBank accession number AJ414699); *Pt*GSTU1 (*Pinus tabulaeformis*, GenBank accession number AY640175); *Ta*GSTU4 (*Aegilops tauschii*, GenBank accession number 1GWCA); *Le*GSTU1 (*Lycopersicon esculentum*, GenBank accession number AY007558); *At*GSTU1 (*Arabidopsis thaliana*, GenBank accession number AF428387); *At*GSTZ1 (*Arabidopsis thaliana,* GenBank accession number NP_178344); *Bn*GSTZ1 (*Brassica napus*, GenBank accession number AAO60042); *Os*GSTZ2 (*Oryza sativa,* GenBank accession number AAK98533); *Ta*GSTZ1 (*Triticum aestivum*, GenBank accession number O04437); *At*GSTF1 (*Arabidopsis thaliana*, GenBank accession number P42760); *Os*GSTF3 (*Oryza sativa*, GenBank accession number AAG32477); *Ta*GSTF2 (*Triticum aestivum*, GenBank accession number CAD29475); *Zm*GSTF1 (*Zea mays*, GenBank accession number XUZM1); *Ee*GSTT1 (*Euphorbia esula*, GenBank accession number AAF64449); *Os*GSTT1 (*Oryza sativa,* GenBank accession number AAK98534) and *At*GSTT10 (*Arabidopsis thaliana*, GenBank accession number CAA10457).

The effect of pH on the enzyme activity was evaluated using GSH and NBD-Cl as substrates. The activity of the recombinant *Os*GSTU17 is pH-dependent (Fig. 6A). The highest activity was observed at pH 7.5. The enzyme still had >50% of its maximum activity at pH 6.5 and 8.5, at pH 5.0 and 9.0 its enzyme activity was abolished. Many plant GSTs show a similar pH profile as *Os*GSTU17 [18,19,24–26], indicating that majority of plant GSTs have high activity in basic solution. The thermal stability of the recombinant *Os*GSTU17 is illustrated in Fig. 6B. *Os*GSTU17 retained 80% of its initial activity at 55 °C, indicating *Os*GSTU17 is stable below 55 °C. Enzyme activity of *Os*GSTU17 at 65 °C was nearly abolished, which is similar to pine tau GSTs [20,27]. As rice often grow in subtropical field, good thermal stability of *Os*GSTU17 may reflect the enzyme's adaptation to the environment.

2.3. Structure prediction and site-directed mutagenesis of the *OsGSTU17*

The three-dimensional structure of *Os*GSTU17 (Fig. 7A) was modelled based on the X-ray structure of the rice *Os*GSTU1 protein (Protein Data Bank code No.: 1OYJ). The structure was further checked by Profile-3D program. Except for residues Asp38, Ala40, Arg216 and Arg217, all other residues of *Os*GSTU17 were scored positive (Fig. 7B), indicating they are reliably folded. The *Os*GSTU17 showed a typical GST structure, and constituted by two distinct domains: a smaller thioredoxin-like N-terminal domain (residues 1–80) and a larger helical C-terminal domain (residues 91–218). N-terminal domain and C-terminal domain were connected by 10-residue linker region (residues 81–90). The N-terminal domain constitutes roughly one-third of the protein and consists of a βαβαββα structural motif in which β3 is antiparallel with respect to the other β-strands (Fig. 7A). The C-terminal domain is composed entirely of six helices (α4 to α9). The α6 helix is disrupted by five amino acids (Phe162, Ala163, Tyr164, Trp165 and Leu166). To keep the naming of the secondary structure consistent with other GST structures the two segments of α6 were named α6' and α6".

Sequence alignment showed that Ser15 of the *Os*GSTU17 is conserved in all plant tau GSTs (Fig. 3). This residue was replaced with an alanine by site-directed mutagenesis in this study. SDS-PAGE showed that the S15A mutant of *Os*GSTU17 was over-expressed in *E. coli* cell (Fig. 4, lane3). MALDI-TOF/MS showed the subunit *Mw* of the S15A mutant was 26.4 kDa (Fig. 5B). Sephadex G-75 gel filtration revealed that the *Mw* of the S15A mutant was approximately 52 kDa (results not shown). Thus, the S15A mutant is a homodimer similar to wild-type protein. ANS is widely used for probing structural changes in proteins [28]. When ANS was bound to the enzymes, the fluorescence intensity was enhanced, accompanied by a blue shift in its fluorescence-emission maximum from 520 nm (free ANS in buffer) to 500 nm for the wild-type and mutant *Os*GSTU17 (Fig. 8). The S15A mutant and wild-type *Os*GSTU17 showed almost identical fluorescence spectra, indicating that S15A mutant shared similar structure with wild-type enzyme. The purified mutant *Os*GSTU17 did not show any GST activity towards the substrates listed in Table 1. However, it was able to bind to GSH-Sepharose 4B affinity matrices, indicating it can bind to GSH substrate.

X-ray structures of wheat *Ta*GSTU4 and rice *Os*GSTU1 (Protein Data Bank code Nos. 1gwc and 1oyj, respectively) show this conserved Ser residue (alignment position 18 in Fig. 3) in *Ta*GSTU4 and *Os*GSTU1 is the catalytic residue responsible for stabilisation of the thiolate anion of enzyme-bound glutathione [6]. Similar to the S15A mutant of *Os*GSTU17, mutant of this conserved Ser residue in pine *Pt*GSTU1 did not show any GSH-conjugating activity, but can bind to GSH affinity columns [19]. A tau GST *Le*GSTU1-1 isolated from tomato has a Gly instead of a Ser at this site [21], and it shows very poor activity in GSH conjugation reactions with CDNB (0.07 μmol/min per mg of protein) but can also bind to GSH substrate [21]. All these findings suggest that, similar to other plant GSTs, the Ser15 residue in *Os*GSTU17 is critical for catalysis.

2.4. Expression pattern of the *OsGSTU17* gene under normal growth conditions and abiotic stresses

To determine the expression pattern of *Os*GSTU17 in different rice tissues, RT-PCR was performed on total RNA isolated from mature leaf, immature leaf, leaf sheath, stem, bud and root tissues, respectively. The RT-PCR results showed that *Os*GSTU17 mRNA was expressed in all tissues (Fig. 9A), indicating that it has a wide distribution and expression in rice, both above and below ground. Constitutive expression of *Os*GSTU17 mRNA in different tissues suggests that this gene plays important biological roles in normal growth conditions.

Fig. 9B shows the relative expression changes for *Os*GSTU17 gene in different tissues after different chemical treatments. In mature leaf, the expression of *Os*GSTU17 mRNA did not change significantly under H_2O_2 and atrazine stresses, but were up-regulated 2-fold in response to CDNB. In immature leaf 2-fold up-regulation of *Os*GSTU17 mRNA was also observed in response to CDNB, but a significant down-regulation in response to H_2O_2 and atrazine. A similar expression pattern was observed in leaf sheath tissue. In stem, the level of *Os*GSTU17 mRNA did not change significantly after CDNB treatment, while a 4- and 33-fold decrease were observed under H_2O_2 and atrazine stresses, respectively. In root tissues, level of *Os*GSTU17 mRNA decreased 2.7-, 1.4- and 4.2-fold after CDNB, H_2O_2 and atrazine treatment, respectively.

The most characteristic function of GSTs is their ability to catalyze the formation of GSH-xenobiotic conjugates, a key step in their

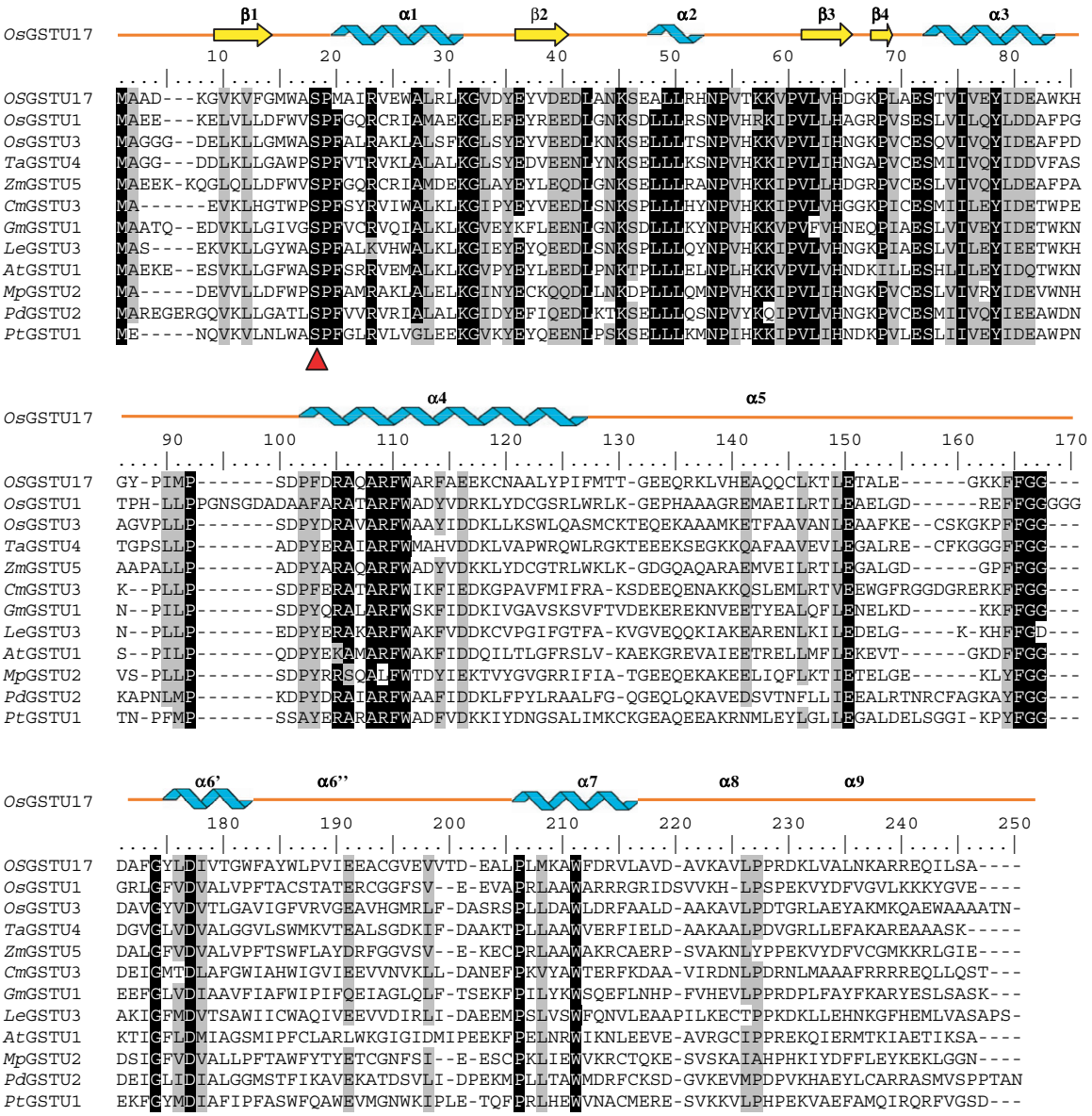

Fig. 3. Sequence alignment of plant tau GSTs and the predicted secondary structure elements of the *Os*GSTU17. Alpha helices and beta strands are represented as helices and arrows, respectively. Conserved residues in all plant tau GSTs are shaded. The mutation site Ser15 of *Os*GSTU17 is marked with ▲ in red. *Os*GSTU1 (*Oryza sativa*, GenBank accession number 1OYJ); *Os*GSTU3 (*Oryza sativa*, GenBank accession number AAG32472); *Ta*GSTU4 (*Aegilops tauschii*, GenBank accession number 1GWCA); *Zm*GSTU5 (*Zea mays*, GenBank accession number CAA73369); *Cm*GSTU3 (*Cucurbita maxima*, GenBank accession number BAC21263); *Gm*GSTU1 (*Glycine max*, GenBank accession number AAA33943); *Le*GSTU3 (*Lycopersicon esculentum*, GenBank accession number AAG16758); *At*GSTU1 (*Arabidopsis thaliana*, GenBank accession number AAL16155); *Mp*GSTU2 (*Malva pusilla*, GenBank accession number AAO61855); *Pd*GSTU2 (*Pinus densata*, GenBank accession number AAY64043) and *Pt*GSTU1 (*Pinus tabulaeformis*, GenBank accession number AAV31760) are included in the alignment.

metabolic detoxification. Because of this detoxification function, plant GSTs have received much attention. Many studies showed that expression of GSTs is enhanced following exposure to a range of xenobiotics and may be induced in response to the general cellular injury and oxidative stress caused by chemical toxins [6,12,14,15,17,23]. In this study, when rice plants were exposed to chemical toxin CDNB, transcript levels of *Os*GSTU17 significantly increased in mature leaf, immature leaf and leaf sheath, indicating that *Os*GSTU17 participated in detoxification metabolism for CDNB.

Plant GST gene families are large and highly diverged. Although some plant GSTs responses to herbicides have been studied extensively [6,14,29,30], their significant and versatile involvements in plant stress responses remain poorly understood. Individual GSTs are differentially regulated in response to many forms of biotic and abiotic stress, suggesting diverse functions in endogenous metabolism. Recently, a study showed that rice *Os*GSTU3 and *Os*GSTU4 could be induced by heavy metal- and hypoxic stress, and they had different responses under salt stress in root [17]. In a phloem-specific rice GST, the expression of the gene was not affected by treatments with pretilachlor and fenclorim [13]. Our study revealed different gene expression patterns of *Os*GSTU17 under different chemical treatments. These case studies gather evidences for diverse regulation mechanisms of GSTs in response to abiotic stresses.

In summary, this study reports the cloning and biochemical and physiological characterization of a GST (*Os*GSTU17) from *O. sativa*. Based on comparative analyses of its amino acid sequence, phylogeny and predicted three-dimensional structure, the *Os*GSTU17 should be classified as a tau class GST. The *Os*GSTU17 showed GSH-conjugating activity with various xenobiotics. Ser15 in the N-terminal domain proved to be a critical catalytic residue,

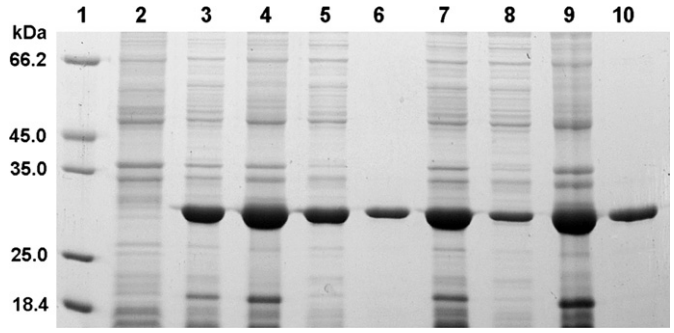

Fig. 4. SDS–PAGE analysis of the recombinant and mutant *Os*GSTU17. Lane 1, molecular mass markers with the sizes shown on the left in kilodaltons; lane 2, total cellular extract from *E. coli* BL21; lanes 3 and 7, total cellular extracts from induced bacteria; lanes 4 and 8, cell pellet after ultrasonication and centrifugation of cells expressing recombinant S15A mutant and wild-type *Os*GSTU17, respectively; lanes 5 and 9, supernatant after ultrasonication and centrifugation of cells expressing recombinant S15A mutant and wild-type *Os*GSTU17, respectively; lanes 6 and 10, the purified recombinant S15A mutant and wild-type *Os*GSTU17, respectively.

responsible for stabilisation of the thiolate anion of enzyme-bound glutathione. Changes over the expression pattern of *Os*GSTU17 suggest possible roles of the gene in detoxification and buffering abiotic stresses. Further investigation on the function of this GST protein may provide new insights into GST evolution, possible detoxification pathways and the significance in plant development.

3. Materials and methods

3.1. Molecular cloning

Based on cDNA sequence of *Os*GSTU17 (GenBank accession no. AF402804), two primers (OsGSTU17-EX1: 5′-TGAATTCATGGCAG-CAGACAAGGGAG-3′, OsGSTU17-EX2: 5′-TAAGCTTTTACTACGCCGA-GAGGATCTGC-3′, EcoRI and HindIII sites underlined, respectively) were designed to amplify the coding region. Total RNA was isolated from rice leave using an Aurum Total RNA Kit (Bio-Rad). The first strand cDNA was synthesized using a TaKaRa RNA PCR Kit (AMV) Ver.3.0 (TaKaRa). PCR was performed in a volume of 25 μl containing about 1 μl of the first strand cDNA, 0.75 U of Taq DNA polymerase (Invitrogen Life Technologies), 200 μM of each dNTP (Invitrogen), 1.5 mM $MgCl_2$ and 10 pmol of each primer (OsGSTU17-EX1 and OsGSTU17-EX2). PCR conditions were optimized to consist of an initial denaturation of 3 min at 95 °C, followed by 35 cycles of 30 s at 94 °C, 40 s at 55 °C and 60 s at 72 °C, and a final extension of 5 min at 72 °C. A PCR product (about 700 bp) was recovered from agarose gel using a GFX PCR DNA and Gel Band Purification Kit (Amersham Pharmacia Biotech), cloned into the pGEM®-T Vector (Promega) and sequenced in both directions. The pGEM®-T Vector containing *Os*GSTU17 cDNA was termed pGEM-T/*Os*GSTU17.

Table 1
Specific activities of the recombinant *Os*GSTU17. The values shown are means ± S.D., calculated from three replicates; ND, no activity detected.

Substrate	Specific activity (μmol/min per mg)
CDNB	0.113 ± 0.019
NBD-Cl	0.203 ± 0.006
NBC	1.153 ± 0.457
DCNB	ND
4-NPA	ND
ECA	ND
Cumene hydroperoxide	0.013 ± 0.002

3.2. Phylogenetic analysis

The protein sequence of *Os*GSTU17 was deduced from the cDNA, aligned with other plant GSTs using ClustalX software [31] and further adjusted manually using BioEdit [32]. Sequence divergence and phylogenetic analysis were performed using MEGA v.4.0 [33]. The neighbour-joining (NJ) method of phylogenetic tree reconstruction was used to establish the genetic relationships between *Os*GSTU17 and other major classes of plant GSTs, with 1000 bootstrap replicates and distant animal GSTs as outgroup using MEGA v.4.0.

3.3. Expression and purification of recombinant *OsGSTU17*

A modified pET30a vector (Fig. 10) was used to express *Os*GSTU17 protein. The plasmid pGEM-T/OsGSTU17 was digested with EcoRI and HindIII, and the resulting fragment was isolated and inserted into the EcoRI and HindIII sites of modified pET30a vector (Fig. 10), which provides the correct reading frame and an only 6×His-tag at the N-terminus. The resultant plasmids were used to

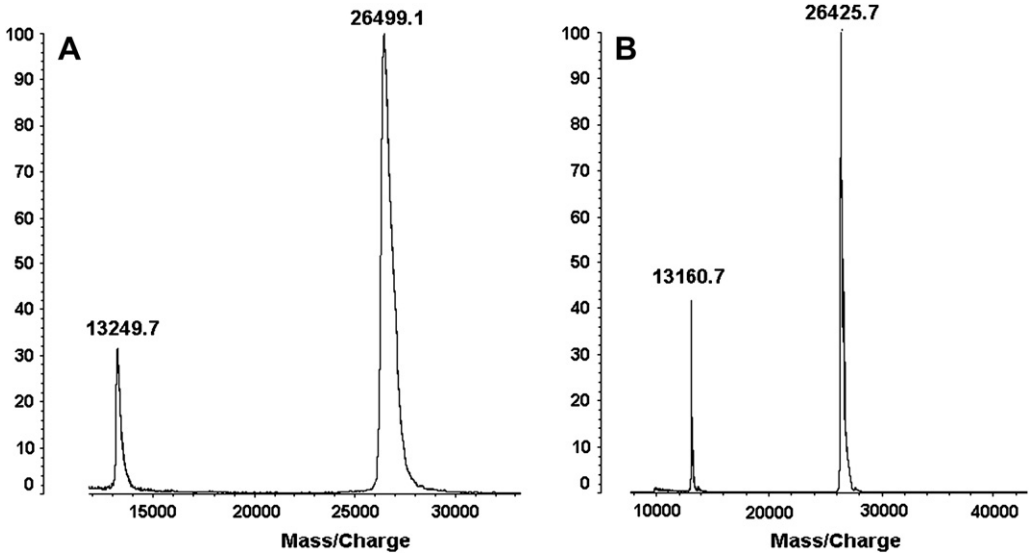

Fig. 5. MALDI-TOF/MS of the purified recombinant *Os*GSTU17 (A) and S15A mutant (B).

Table 2
Kinetic constants of the purified recombinant *Os*GSTU17 using NBD-Cl and GSH as substrates.

Substrate	K_m (mM)	V_{max} (μmol/min per mg)	k_{cat} (min^{-1})	k_{cat}/K_m (mM^{-1} min^{-1})
NBD-Cl	0.324 ± 0.016	0.219 ± 0.006	0.257	0.793
GSH	0.058 ± 0.006	0.225 ± 0.011	0.264	4.552

transform *E. coli* BL21. Colonies containing the appropriate insert were identified by sequencing.

An overnight culture of *E. coli* BL21 transformed with plasmid ΔpET30a/OsGSTU17 was diluted 1:100 and grown until the optical density (A_{600}) reached 0.5. Isopropyl-β-D-thiolactopyranoside (IPTG) was added to the culture at a final concentration of 0.1 mM and incubation was continued for a further 16 h at 37 °C. Bacteria were harvested by centrifugation at 5000 *g* for 3 min at 4 °C, resuspended in binding buffer (20 mM sodium phosphate, 0.5 M NaCl, 20 mM imidazole, pH 7.4), and disrupted by cold sonication. The homogenate was then subjected to centrifugation at 10 000 *g* for 10 min at 4 °C. The resultant particulate material and a small portion of the supernatant were analyzed by sodium dodecyl sulfate polyacrylamide gel electrophoresis (SDS-PAGE). The rest of the supernatant was loaded onto a Ni Sepharose High Performance column (Amersham Pharmacia Biotech) that had been pre-equilibrated with binding buffer. The over-expressed protein that bound to the Ni Sepharose High Performance column was eluted with elution buffer (20 mM sodium phosphate, 0.5 M NaCl, 500 mM imidazole, pH 7.4). The purified recombinant protein was desalted using a PD-10 column (Amersham Pharmacia Biotech) in 10 mM Tris–HCl buffer, pH 7.4.

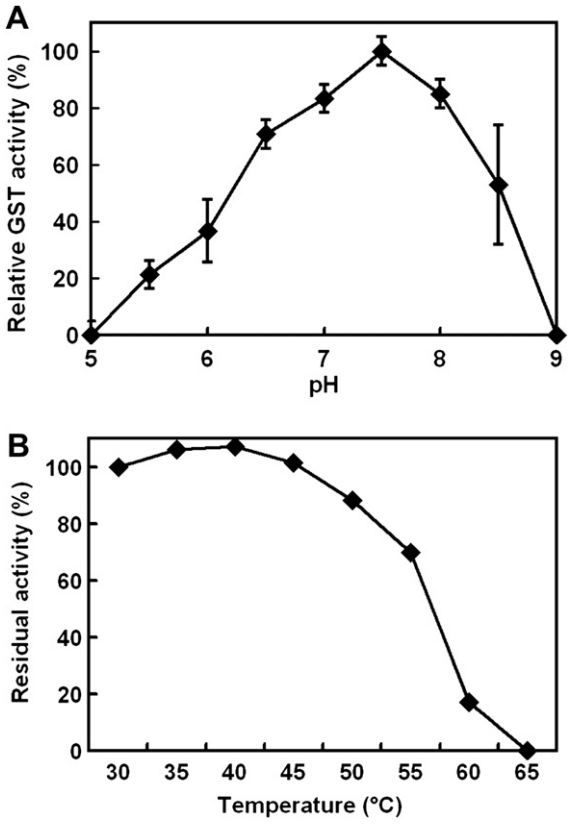

Fig. 6. Effect of pH on CDNB-conjugating activities of OsGSTU17 (A). Thermal stability of OsGSTU17 (B), based on the retention of enzymatic activity towards the substrate NBD-Cl following heat treatment.

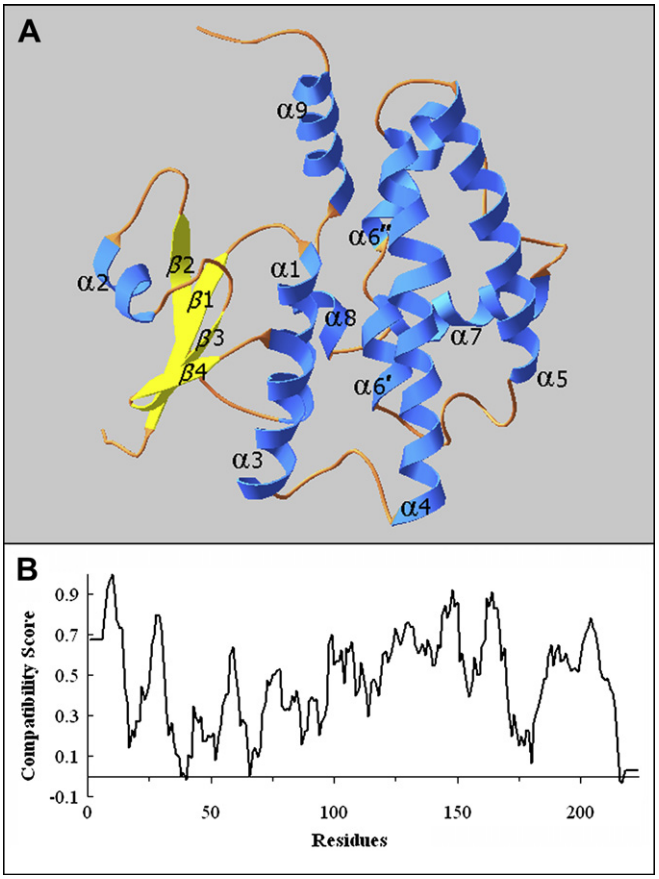

Fig. 7. Predicted three-dimensional structure of *Os*GSTU17 (A) and the evaluation of the *Os*GSTU17 structure by Profile-3D program (B). Alpha helices and beta strands are represented as blue helices and yellow arrows in A, respectively. The three-dimensional structural image was generated using the program Swiss-Pdb Viewer.

3.4. Mutagenesis of the OsGSTU17 gene

Sequence alignment showed that Ser15 of the *Os*GSTU17 is conserved in all plant tau GSTs (Fig. 3). To investigate whether the conserved Ser15 residue is important for catalysis, Ser15 was replaced with an alanine residue by site-directed mutagenesis. The cDNA encoding *Os*GSTU17 in pGEM-T/OsGSTU17 was used as a template in the site-directed mutagenesis. The mutagenic primer 5′-TGAATTCATGGCAGCAGACAAGGGAGTGAAGGTGTTCGGCATGTGGGCGGCCCCCATGG-3′ (EcoRI site underlined, and the Ser15 site shadowed) was designed to replace the Ser15 with an alanine residue in the *Os*GSTU17 gene. The PCR product was cloned and expressed as described in the

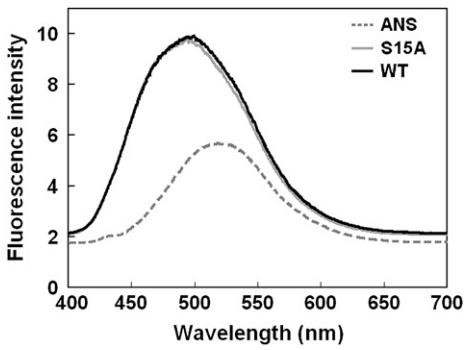

Fig. 8. Fluorescence-emission spectra of ANS binding to the S15A mutant and wild-type *Os*GSTU17.

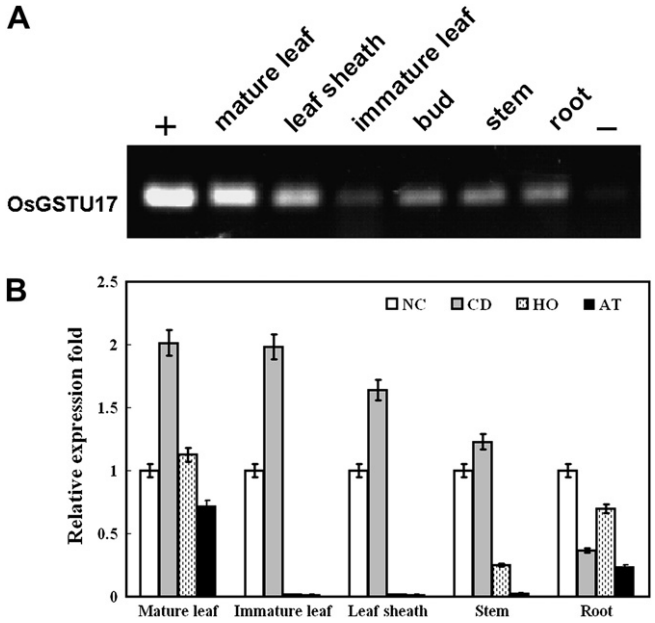

Fig. 9. Expression of the *Os*GSTU17 gene. Expression of the *Os*GSTU17 gene in different tissues of rice under normal growth condition as revealed by RT-PCR (A). (+) positive control using the construct pGEM-T/OsGSTU17 as PCR template; (−) negative control using RT-PCR reaction without template. qRT-PCR analysis of transcript levels of the *Os*GSTU17 gene under abiotic stresses (B). The *Y* axis indicates the expression level relative to the control (NC). The rice plants were grown under normal growth conditions (NC), 1.0 mM CDNB (CD), 5.0% H_2O_2 (HO), and 1.5% Atrazine (AT) treatment, respectively. All data are presented as means of five independent experiments. Bars show means ± SD ($n = 5$).

subsection above, and the mutant (S15A) was confirmed by DNA sequencing. *E. coli* BL21 cells transformed by the ΔpET30a/OsGSTU17 mutant were induced by IPTG under the same conditions as for cells transformed by wild-type pET30a/OsGSTU17. The crude extracts were purified using Ni Sepharose High Performance column, as above.

3.5. Enzyme assays and kinetic studies

GST activities towards 1-chloro-2, 4-dinitrobenzene (CDNB), ethacrynic acid (ECA) and p-nitrophenyl acetate (4-NPA) were measured as described by Habig et al. [34], and activity towards 7-chloro-4-nitrobenzo-2-oxa-1, 3-diazole (NBD-Cl) as described by Ricci et al. [35]. Ativity towards cumene hydroperoxide was measured as described by Edwards and Dixon [36]. To accurately determine the subunit *Mw* of the recombinant enzyme, the purified recombinant protein was denatured in 8.0 M urea and then analyzed on a Bruker Biflex-III MALDI/TOF mass spectrometer (Bruker Analytical Systems). The molecular weight of the purified recombinant *Os*GSTU17 and the mutant were estimated by gel filtration on a Sephadex G-75 column using the following molecular weight standards: bovine serum albumin (66 kDa), ovalbumin (45 kDa) and trypsin inhibitor (22 kDa). Protein concentrations were determined by measuring absorbance at 280 nm. The dependence of GST activity on pH was measured according to Yuen et al. [37]. Thermal stability measurements of the purified *Os*GSTU17 were carried out by incubating the samples for 15 min at various temperatures from 25 °C to 65 °C at 5 °C intervals. GST activity towards NBD-Cl was determined at the end of each incubation.

The fluorescence dye 8-anilino-1-naphthalene-sulfonate (ANS) is a valuable probe for the detection and analysis of structural changes in proteins [28]. In order to detect structural changes between the mutant and wild-type enzymes, the ANS (1-anilino-8-naphthalene-sulfonate) binding assay was monitored using a HITACHI F-4500 FL Spectrophotometer. 100 μl of 2 mM ANS was added to a final concentration of 0.05 mg/ml enzyme (1 M sodium phosphate buffer, pH 6.5) in a 1 ml reaction mixture. A total of three scans each for blank and sample were recorded and averaged for each enzyme. Reported spectra are the means from at least three independent experiments.

The apparent K_m and V_{max} values for GSH were determined using a GSH range from 0.2 to 1.0 mM and a fixed NBD-Cl concentration of 1.0 mM. The apparent K_m and V_{max} values for NBD-Cl were determined using an NBD-Cl range from 0.04 to 0.8 mM and a fixed GSH concentration of 1.0 mM. The kinetic parameters were derived using non-linear regression analysis of Hyper32 program available at http://www.liv.ac.uk/~jse/software.html.

3.6. Homology modelling

Protein Data Bank structure 1OYJ [PDB] was used as template for constructing a structure model of *Os*GSTU17. Sequences were aligned using Align 2D structure alignment program (Homology Module, InsightII). Structures were built using the modeler module of InsightII. All Structures were verified by profile-3D program in InsightII. The models were selected according to model evaluation score calculated by Profile-3D.

3.7. Chemical treatments and qPT-PCR

To investigate the induced expression levels of the *Os*GSTU17, rice plants were treated with different chemicals. Rice seedlings were grown individually in 10 cm × 10 cm pots for three months, then irrigated and sprayed with 1.0 mM CDNB, 5.0% H_2O_2 and 1.5% Atrazine solution, separately. Each treatment was conducted in five replicate plants. 12 h after the chemical treatments, total RNA was isolated from mature leaf, immature leaf, leaf sheath, stem and root tissues of each rice seedling.

Reverse transcription PCR (RT-PCR) was performed using an TaKaRa RNA PCR Kit (AMV) Ver.3.0 (TaKaRa). Quantitative RT-PCR was performed on a Mx3000P real-time PCR system (Stratagene) using the RT-PCR products as templates. Brilliant SYBR Green QPCR Master Mix (Stratagene) was used in all qPCR reactions. Two specific primers for *Os*GSTU17 were used: OsGSTU17-RT1 (5′-CTGAAGAGA AGTGCAACGCTG-3′) and OsGSTU17-RT3 (5′-CGAGAGGATCTGCTCAC GG-3′). The qPCR conditions were optimized to comprise an initial denaturation step of 10 min at 94 °C followed by 40 cycles of 94 °C for

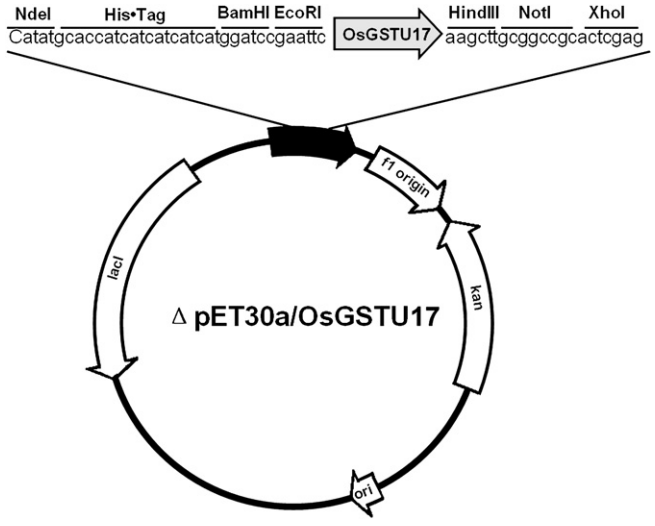

Fig. 10. Construction of *Os*GSTU17 expression plasmid.

30 s, 60 °C for 45 s and 72 °C for 30 s. A melt-curve analysis immediately followed amplification at 94 °C for 60 s, cooling to 60 °C for 30 s, and a slow rise in temperature to 94 °C with continuous acquisition of fluorescence decline. Melt-curve analysis is used to observe melting characteristics of the amplicon. It is performed immediately after amplification to determine the presence of the specific product. The rice actin gene (Os03g0718100) was used as an internal control in qPCR analysis with the primer sequences for actin cDNA as: forward: 5′-CTTCTACAACGAGCTCCGTGTG-3′, reverse: 5′-TCCAACACAATACCTGTGGTACG-3′. Standard curve based on threshold cycles was constructed for each reaction by using a 10-fold dilution series of *Os*GSTU17 cDNA. Samples were run in duplicate and the template quantity was estimated from threshold cycles compared to the standard curve. The quantification data were normalized to actin mRNA expression level.

Acknowledgments

This study was supported by grants from the Natural Science Foundation of China (NSFC 30770149), the National Basic Research Program of China (2009CB119104) and the Chinese Academy of Sciences (KZCX2-YW-414).

References

[1] D. Sheehan, G. Meade, V.M. Foley, C.A. Dowd, Structure, function and evolution of glutathione transferases: implications for classification of non-mammalian members of an ancient enzyme superfamily, Biochem. J. 360 (2001) 1–16.
[2] R. Edwards, D.P. Dixon, V. Walbot, Plant glutathione S-transferases: enzymes with multiple functions in sickness and in health, Trends Plant Sci. 5 (2000) 193–198.
[3] C. Frova, The plant glutathione transferase gene family: genomic structure, functions, expression and evolution, Physiol. Plant 119 (2003) 469–479.
[4] C. Frova, Glutathione transferases in the genomics era: new insights and perspectives, Biomol. Eng. 23 (2006) 149–169.
[5] B. McGonigle, S.J. Keeler, S.M. Lau, M.K. Koeppe, D.P. O'Keefe, A genomics approach to the comprehensive analysis of the glutathione S-transferase gene family in soybean and maize, Plant Physiol. 124 (2000) 1105–1120.
[6] R. Thom, I. Cummins, D.P. Dixon, R. Edwards, D.J. Cole, A.J. Lapthorn, Structure of a tau class glutathione S-transferase from wheat active in herbicide detoxification, Biochemistry 41 (2002) 7008–7020.
[7] G.K. Agrawal, N.-S. Jwa, R. Rakwal, A pathogen-induced novel rice (*Oryza sativa* L.) gene encodes a putative protein homologous to type II glutathione S-transferases, Plant Sci. 163 (2002) 1153–1160.
[8] L. Loyall, K. Uchida, S. Braun, M. Furuya, H. Frohnmeyer, Glutathione and a UV light-induced glutathione S-transferase are involved in signaling to chalcone synthase in cell cultures, Plant Cell 12 (2000) 1939–1950.
[9] B. Ezaki, M. Suzuki, H. Motoda, M. Kawamura, S. Nakashima, H. Matsumoto, Mechanism of gene expression of *Arabidopsis* glutathione S-transferase, *AtGST1*, and *AtGST11* in response to aluminum stress, Plant Physiol. 134 (2004) 1672–1682.
[10] I.C. Chen, I.C. Huang, M.J. Liu, Z.G. Wang, S.S. Chung, H.L. Hsieh, Glutathione S-transferase interacting with far-red insensitive 219 is involved in phytochrome A-mediated signaling in *Arabidopsis*, Plant Physiol. 143 (2007) 1189–1202.
[11] J.R. Wu, C.L. Cramer, K.K. Hatzios, Characterization of two cDNAs encoding glutathione S-transferases in rice and induction of their transcripts by the herbicide *safener fenclorim*, Physiol. Plant 105 (1999) 102–108.
[12] D.E. Riechers, G.P. Irzyk, S.S. Jones, E.P. Fuerst, Partial characterization of glutathione S-transferases from wheat (*Triticum* spp.) and purification of a safener-induced glutathione S-transferase from *Triticum tauschii*, Plant Physiol. 114 (1997) 1461–1470.
[13] A. Fukuda, Y. Okada, N. Suzui, T. Fujiwara, T. Yoneyama, H. Hayashi, Cloning and characterization of the gene for a phloem-specific glutathione S-transferase from rice leaves, Physiol. Plant 120 (2004) 595–602.
[14] F. Xu, E.S. Lagudah, S.P. Moose, D.E. Riechers, Tandemly duplicated Safener-induced glutathione S-transferase genes from *Triticum tauschii* contribute to genome- and organ-specific expression in hexaploid wheat, Plant Physiol. 130 (2002) 362–373.
[15] L. Scarponi, E. Quagliarini, D. Del Buono, Induction of wheat and maize glutathione S-transferase by some herbicide safeners and their effect on enzyme activity against butachlor and terbuthylazine, Pest Manag. Sci. 62 (2006) 927–932.
[16] N. Soranzo, M. Sari Gorla, L. Mizzi, G. De Toma, C. Frova, Organisation and structural evolution of the rice glutathione S-transferase gene family, Mol. Genet. Genomic. 271 (2004) 511–521.
[17] A. Moons, *Osgstu3* and *osgtu4*, encoding tau class glutathione S-transferases, are heavy metal- and hypoxic stress-induced and differentially salt stress-responsive in rice roots, FEBS Lett. 553 (2003) 427–432.
[18] H.Y. Cho, S.Y. Yoo, K.H. Kong, Cloning of a rice tau class GST isozyme and characterization of its substrate specificity, Pest Biochem. Physiol. 86 (2006) 110–115.
[19] Q.Y. Zeng, H. Lu, X.R. Wang, Molecular characterization of a glutathione transferase from *Pinus tabulaeformis* (Pinaceae), Biochimie 87 (2005) 445–455.
[20] Q.Y. Zeng, X.R. Wang, Divergence in structure and function of tau class glutathione transferase from *Pinus tabulaeformis, P. yunnanensis and P. densata*, Biochem. Syst. Ecol. 34 (2006) 678–690.
[21] K.G. Kilili, N. Atanassova, A. Vardanyan, N. Clatot, K. Al-Sabarna, P.N. Kanellopoulos, A.M. Makris, S.C. Kampranis, Differential roles of tau class glutathione s-transferases in oxidative stress, J. Biol. Chem. 279 (2004) 24540–24551.
[22] D.P. Dixon, D.J. Cole, R. Edwards, Dimerisation of maize glutathione transferases in recombinant bacteria, Plant Mol. Biol. 40 (1999) 997–1008.
[23] I. Cummins, D. O'Hagan, I. Jablonkai, D.J. Cole, A. Hehn, D. Werck-Reichhart, R. Edwards, Cloning, characterization and regulation of a family of phi class glutathione transferases from wheat, Plant Mol. Biol. 52 (2003) 591–603.
[24] P. Schroder, H. Rennenberg, Characterization of glutathione S-transferase from dwarf pine needles (*Pinus mugo* Turra), Tree Physiol. 11 (1992) 151–160.
[25] S.H. Hong, H.J. Park, K.H. Kong, Purification and biochemical properties of glutathione S-transferase from *Oryza sativa*, Comp. Biochem. Physiol. B 122 (1999) 21–27.
[26] G.P. Irzyk, E.P. Fuerst, Purification and characterization of a glutathione S-transferase from benoxacor-treated maize (*Zea mays*), Plant Physiol. 102 (1993) 803–810.
[27] Q.Y. Zeng, X.R. Wang, Catalytic properties of glutathione-binding residues in a tau class glutathione transferase (PtGSTU1) from *Pinus tabulaeformis*, FEBS Lett. 579 (2005) 2657–2662.
[28] E. Schonbrunn, S. Eschenburg, K. Luger, W. Kabsch, N. Amrhein, Structural basis for the interaction of the fluorescence probe 8-anilino-1-naphthalene sulfonate (ANS) with the antibiotic target MurA, Proc. Natl. Acad. Sci. U.S.A. 97 (2000) 6345–6349.
[29] B.P. DeRidder, D.P. Dixon, D.J. Beussman, R. Edwards, P.B. Goldsbrough, Induction of glutathione S-transferases in *Arabidopsis* by herbicide safeners, Plant Physiol. 130 (2002) 1497–1505.
[30] E.P. Fuerst, G.P. Irzyk, K.D. Miller, Partial characterization of glutathione S-transferase isozymes induced by the herbicide *safener benoxacor* in maize, Plant Physiol. 102 (1993) 795–802.
[31] J.D. Thompson, T.J. Gibson, F. Plewniak, F. Jeanmougin, D.G. Higgins, The Clustal X windows interface: flexible strategies for multiple sequence alignment aided by quality analysis tools, Nucleic, Acids. Res. 24 (1997) 4876–4882.
[32] T.A. Hall, BioEdit: a user-friendly biological sequence alignment editor and analysis program for Windows 95/98/NT, Nucleic. Acids. Symp. Ser. 41 (1999) 95–98.
[33] K. Tamura, J. Dudley, M. Nei, S. Kumar, MEGA4: molecular evolutionary genetics analysis (MEGA) software version 4.0, Mol. Biol. Evol. 24 (2007) 1596–1599.
[34] W.H. Habig, M.J. Pabst, W.B. Jakoby, Glutathione S-transferases. The first enzymatic step in mercapturic acid formation, J. Biol. Chem. 249 (1974) 7130–7139.
[35] G. Ricci, A.M. Caccuri, M. Lo Bello, A. Pastore, F. Piemonte, G. Federici, Colorimetric and fluorometric assays of glutathione transferase based on 7-chloro-4-nitrobenzo-2-oxa-1,3-diazole, Anal. Biochem. 218 (1994) 463–465.
[36] R. Edwards, D.P. Dixon, Plant glutathione transferases, Methods. Enzymol. 401 (2005) 169–186.
[37] W.K. Yuen, J.W. Ho, Purification and characterization of multiple glutathione S-transferase isozymes from *Chironomidae larvae*, Comp. Biochem. Physiol. A 129 (2001) 631–640.